Iranian Journal of Organic Chemistry Vol. 14, No. 4 (2022) 3465-3474

Evaluation of adsorption potential of Buprenorphine drug from blood plasma by its molecular imprinted polymer; a joint experimental and theoretical study

Maryam Khanlari[a], Bahram Daraei[b*], Leila Torkian[a,c*], Maryam Shekarchi [d], Mohammad Reza Manafi[a]

[a]*Department of applied Chemistry, South Tehran Branch, Islamic Azad University, Tehran, Iran*
[b]*Department of Toxicology and pharmacology, School of pharmacy, Shahid Beheshti University of Medical Sciences, Tehran, Iran*
[c]*Research Center of Modeling and Optimization in Science and Engineering, Islamic Azad University, South Tehran Branch, Tehran, Iran*
[d]*Food and Drug Laboratory Research Centre, Food and Drug Organization, MOH&ME, Tehran, Postal code: 1113615911, Iran.*

Received: September 2022; Revised: September 2022; Accepted: October 2022

Abstract: In this paper, we have described the use a molecular imprinted polymer (MIP) templated with Buprenorphine (BUP) drug for adsorption of its residue from the biological samples. Preparing this MIP by BUP (as the molecular template) causes to formation of billions of special active sites, which only accept this drug as the guest. Thus, this MIP could absorb BUP from the system in different conditions. The successful use of such MIPs in adsorption BUP from the blood which is described in this work, shows the possibility of using this sorbent, in solid phase extraction, in adsorption/removal, and in drug delivery application of this important drug in the human blood plasma. To do this, after preparing the mentioned MIP, the adsorption process of the drug was investigated by HPLC system. In addition, the results have showed that the obtained MIP is a suitable candidate for the solid phase adsorption of the drug from the blood plasma. Also, the collected data showed that using the MIP is more suitable compared to NIP in the examined processes. Moreover, both of the MIP-, and non-imprinted polymers (NIP)-drug systems were designed and optimized by light of the density functional theory (DFT) approach. The reached results showed that the theoretical calculations would support the experimental data, confirming the priority of adsorption of the drug by MIP compared to NIP.

Keywords: Molecular imprinted polymer, Buprenorphine, Density functional theory, Solid phase extraction, Drug delivery

Introduction

One of the most important opioids, which would relieve severe pains like the cancer related ailments, is Buprenorphine (BUP). In this regard, several forms of formulations containing the liquid forms, and the controlled-release tablets have been commercially released for BUP drug [1]. Optimization of the adsorption process of the drug from the blood has always been important for the experts. It will be more important when the measuring of the bioavailability, the release rate, and the shelf life of a drug is required [2].

During decades, several approaches were designed for optimization of the adsorption as well as the release processes of the drugs such as osmotic pumps [3], slow-release tablets [4], the molecular imprinted polymers (MIPs) [5], and the sol-gels [6].

In this regard, the molecular imprinting technology (MIT), has been recently developed to solve the problems in different related area. It should be mentioned that the MIPs, as the best products of this technology, have been considered as candidates for drug delivery systems or solid phase extraction processes [7]. To prepare MIPs, the polymer materials are obtained in presence of a molecular compound as template (Figure 1). After synthesizing the polymer, it

*Corresponding author. E-mail: bdaraei@sbmu.ac.ir, ltorkian@azad.ac.ir

was washed for several times to make the composition free of those template molecules. Therefore, the matrix is full of free positions, which could receive that especial molecular compound for further use [8]. Obviously, such hosts in the MIP could be used as the stationary phase for the packing of the chromatography columns [9], as the nano sized actuators [10], as nano sorbents [11], as the biosensors [12], and also as new tiny drug release systems [13].

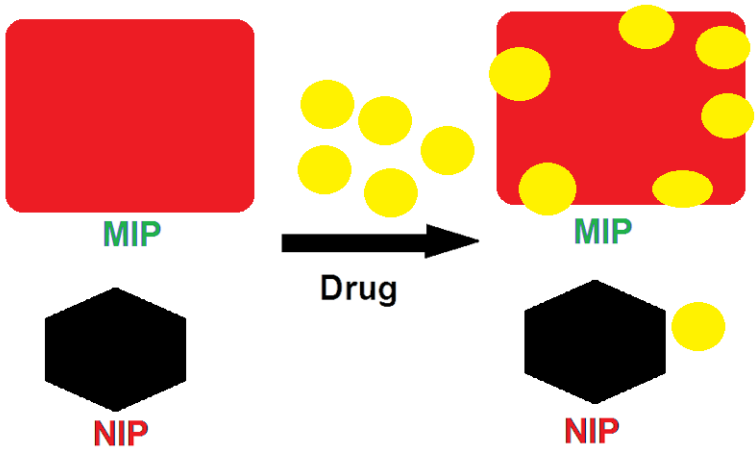

Figure 1. The absorption process of BUP by MIP host compared to NIP as reference

Using MIPs, in one hand, formulators could optimize certain dosages of the drugs and regulate the release rates of the drugs [14] which would be considered as key advantage of such technique. On the other hand, analysts could use MIPs as suitable devices for solid phase extractions of the drugs from the solutions like the biological ones.

Due to these, in the present work, we have used BUP drug as the molecular template for preparing the MIP for application in the solid phase extraction of this drug from the human blood plasma. The scanning electron microscopy (SEM) was used to morphology investigation and nano-scaling analysis. The drug adsorption behavior of the composites in the real biological environment was studied by high performance chromatography (HPLC) [15,16]. Thus, the main aim of this work was to evaluate the drug adsorption ability of MIP from the real samples. The results of the work showed that using the MIP for this purpose was more suitable than that of NIP. Moreover, both of the MIP, and NIP-drug complexes were designed and optimized by applying the density functional theory (DFT) method. The results indicated that the theoretical calculations support the experimental data, confirming the favorability of adsorption of the drug by the MIP compared to the NIP as reference.

Results and discussion

Structural characterization of the MIP-BC

FT-IR spectroscopic analysis

The FT-IR spectrum of BUP free-MIP, and the BUP loaded MIP, were recorded to confirm the synthesis of MIP. In the BUP free-MIP, there are strong absorption peaks at about *ν*C=O (stretching)=1729 cm^{-1}, *ν*C-O (stretching)=1259 cm^{-1}, and *ν*O-H (stretching)= 3436 cm^{-1}, due to the OH bonds, and the carboxyl groups from the MAA (functional monomer), and EGDMA (cross-linking agent).

By comparison, after loading BUP on the MIP, the absorption peaks of C=O, C-O, and O-H, shifted to about 1733 cm^{-1}, 1258 cm^{-1}, and 3424 cm^{-1}, respectively. Moreover, the intensity of absorption peak of the O-H bond has increased at 3434 cm^{-1} in the BUP loaded MIP, which reveals of formation of a hydrogen bond between BUP and MIP.

Physiochemical properties of MIP-BC composite

The results of the swelling analysis indicated that its value for MIP (containing 20 mg MIP+BC) is about 54.38%. While, its amount for NIP (containing 20 mg NIP) is only about 40.76%. It showed that there is a systematic arrangement of billions of active sites in MIP compared to NIP.

Morphological structure analysis

As shown in Figure **2**, both the surface of the NIP, and MIP are probed by applying the SEM photographs. These figures confirm that both NIP and MIP particles have almost uniform structures and spherical morphologies. Moreover, the results indicate that the average particle sizes are lower than 100 nm, both for NIP, and MIP, respectively. In addition, the SEM images confirm the uniform and regular texture of the nanocomposite. It indicates that NIPs and MIPs are in nano dimensions, due to their nano scale diameters. Also, there is no considerable difference in the morphology of surfaces between the MIP, and NIP. Therefore, the loading of BUP on the polymer or applying it as the molecular template for the synthesis of MIP does not lead to a considerable change on its surface morphology of the sorbents. Hence, the oligomerization of the composite has been observed in some parts of the images. These observations might be due to the tendency for oligomerization and the increase in surface reactivity in such nano-sized processing.

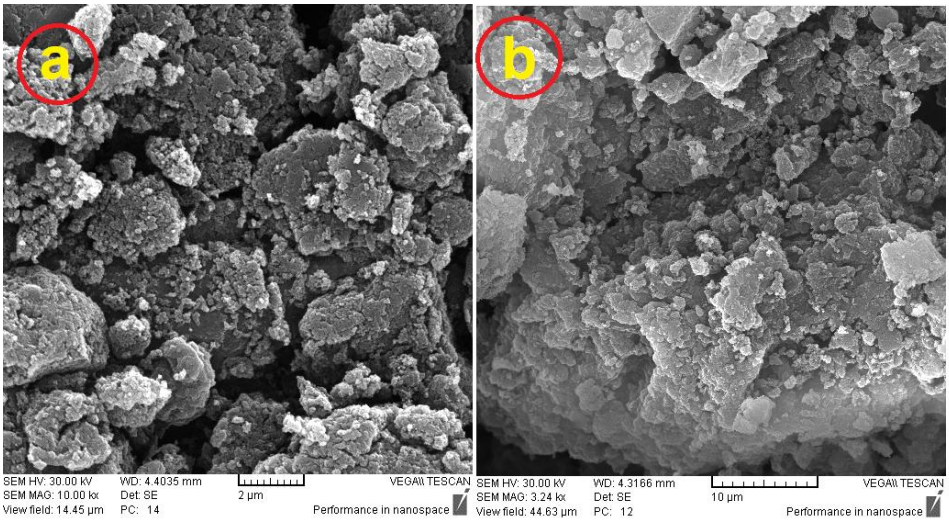

Figure 2. The SEM images of NIP nano particles (A), and MIP nano particles (B)

Adsorption behaviors of MIP

Determination of the adsorption kinetics

During the kinetic analyses, different models were drawn to investigate the most trustable patterns. As given in Figure 3, Table 1, the most linearity was detected in the case of the Longmire expression plot (part a). It indicates that the adsorption of the drug from the plasma as a square root of time could be explained by the physicochemical properties of BUP as a relatively polar drug. Such forms could enhance the drug adsorption from some solutions like blood plasma. Those could also control the drug release from the sorbent. To mimic the real conditions of the human environment, and to investigate the release behavior of BUP in the drug-loaded MIP, the absorption experiments were performed in the pH=7.4 (which is the pH of the human blood serum. Moreover, the solution was studied under continuous stirring at 37 ± 0.5 ◦C (the human body's normal temperature). The results given in Table 1, indicates that the adsorption process of BUP by MIP and NIP follow the Longmire adsorption isotherm due to its regression coefficient (R^2 ≥0.91) which is more closed to 1. Obviously, it is significantly trustable than those of Temkin (R^2 ≥0.61), and Freundlich (R^2 ≥0.59). Thus, the chemical adsorption of BUP on the sites and surfaces of the MIP occurs based on single layer adsorption on homogenic substrates. Also, the data of Table 2 related to the effect of changes of the BUP drug concentration on the adsorption process reveal that in the case of NIP as sorbent, by increasing the BUP concentration up to 60 µg ml^{-1}, the adsorption percentage significantly increases (from 35.01% at 10 µg ml^{-1} to 60.04% at 60 µg ml^{-1}); while, at concentrations higher than 60 µg ml^{-1}, the adsorption percentage decreases (down to 25.05% at 120 µg ml^{-1}). In the case of MIP as sorbent, the pattern of adsorption changes by the drug concentration is similar to NIP. Hence, the gap between the adsorption percentages from 10 µg ml^{-1}

(98.21%) to 60 µg ml^{-1} (98.44%) is considerably lower than the same gap of NIP. It shows that unlike NIP, adsorption of BUP by MIP is approximately independent of the drug concentration.

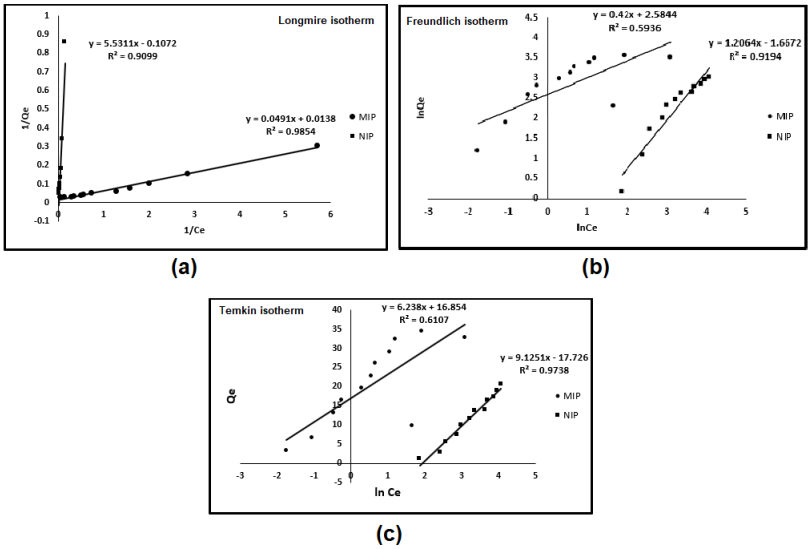

Figure 3. The Longmire (a), Freundlich (b), and Temkin (c) isotherms for adsorption of BUP by MIP and by NIP

Table 1. the values of the parameters related to the adsorption isotherms of BUP by the selected sorbents

Models	**Temkin**			**Freundlich**			**Longmire**			
Items	A	B	R^2	K_f	n	R^2	$q_{e,max}$	R_L	K_L	R^2
MIP	6.24	1.86	0.61	13.25	2.38	0.59	5.53	0.16	0.11	0.91
NIP	9.13	1.73	0.97	5.30	0.83	0.92	0.05	0.59	0.14	0.98

Table 2. Adsorption percentages of the drug by MIP, and NIP, at different concentrations.

Concentration (µg/ml)-NIP (n=3)	q_e (mg/g)-NIP	Adsorption (%)- NIP	Concentration (µg/ml)- MIP (n=3)	q_e (mg/g)-MIP	Adsorption (%)- MIP
10	1.16	35.01	10	3.275	98.21
20	2.93	44.05	20	6.55	98.25
40	5.57	55.66	40	9.83	98.34
50	7.33	55.00	50	13.12	98.42
60	10.00	60.04	60	16.41	98.44
70	11.67	58.33	70	19.55	97.76
80	13.67	58.57	80	22.74	97.47
90	14.07	56.55	90	26.01	97.53
100	16.33	54.44	100	29.04	96.81
120	17.33	52.05	120	32.22	81.66

Adsorption of BUP from the blood plasma by MIP

Table 3 represents validation results of this solid phase extraction based on the concentrations of the BUP drug which was absorbed by MIP and by NIP nanoparticles from the different concentrations of the standard solution prepared from blood plasma. First observable outcome of the data is the higher ability of the MIP compared to NIP for adsorption of BUP. Somehow, at the least concentration (10 µg ml^{-1}), the percentage of adsorption of the drug by MIP is 98.9% which is higher than that of NIP (37.8%). In addition, by increasing the concentration of the drug in the plasma, the adsorption percentage slightly decreases; somehow, the minimum adsorption for MIP (89.0%) occurs in 40 µg ml^{-1}. While, at this concentration (40 µg ml^{-1}), the adsorption percentage of NIP is only 33.9%. Thus, in higher concentrations, the amounts of this value slightly decrease.

Table 3. the key validation factors related to accuracy and precision of BUP adsorption from the protein-free blood plasma

Compound	**Concentration (ng/mL)**	**Accuracy (%)**		**Precision (RSD %)**	
		MIP	NIP	Intra-day	Inter- day
Buprenorphine	10	98.9±5.1	37.8±4.5	.1°	4.51
	20	92.1±1.7	29.8±5.9	1.7	5.99
	40	89.0±2.8	33.9±6.5	2.8	5.56

Theoretical calculations and the binding energies

Beside the experimental results, the quantum chemical calculations were aided to give a better understanding about the interactions between the host (sorbents) and the guest (BUP drug). Using it, researchers are able to investigate the molecular and atomic behaviors of sub-molecular fragments and the other reactive species. Therefore, we have drawn each of the isolated species containing the BUP drug, MIP, and NIP for the first step. Then, the designed geometrical structures were putted under quantum chemical calculations to give any meta-stable species as the optimized output files. Then, the optimized geometry of BUP was putted closed to each of the sorbents to give the host-drug systems. Next, the energy saddles of the best geometries were found, and the theoretical level of calculation were evaluated to the B3LYP/6-31G(d) level of theory. Also, the structural parameters, the atomic orientations, the PES carves, Mulliken charges, and the results of FMO calculations were extracted, which showed good agreements with the experimental observations. Both the experimental and the theoretical results revealed about the strong interactions between the MIP as sorbent and the BUP drug. The data represented in Figure **4**, showed that there are only one hydrogen bond (H2-O41 with 1.90 Å) in the BUP-NIP system; while, there are several hydrogen bonds and interactions between the conjugated MIP-BUP system (like H6-O7= 1.81 Å; H4-O5= 1.93 Å; H2-O1=1.77 Å; H4-O3= 2.62 Å). The considerably higher amounts of hydrogen bonding between the MIP (host) and BUP drug (guest) compared to the NIP-BUP system, confirmed the strong interaction in the MIP-BUP complex. Also, the H2-O3 phenolic hydrogen bond length slightly increased from 0.98 Å in the NIP-BUP to 0.99 Å in the MIP-BUP complex, indicating more interaction of the BUP drug in its MIP complex, compared to its NIP complex form. In the case of the energy changes, the results of the PES calculations (Figure 5) indicated that the absorption of BUP by the MIP as the host, releases an amount of -16.23 kcal mol-1 which was considerably higher than that of adsorption of NIP by BUP. Therefore, the PES studies confirmed that the absorption process of BUP by the MIP is more favorable compared to NIP in view of thermodynamics. Thus, these results confirm the outcome of the theoretical calculations of the structural analysis in fast adsorption of BUP by the MIP which

was in agreement with experimental results. As given in Figure 6, the frontier molecular orbitals (FMOs) distributions show that in the MIP-BUP system, the LUMO, and HOMO orbitals are mainly placed on the rings of BUP (guest) side. Somehow, there is not any observable sign of FMOs in the host. Hence, the in case of the NIP-BUP system, small parts of FMOs could be detected in the host (NIP). In addition, in the case of the guest (BUP), major parts of FMOs could be found in the aromatic rings and in its adjacent cycle. In one hand, it indicates that there are not a significant electron transfer or covalent bond formation between the sorbent and the BUP drug. On the other hand, such FMO arrangements reveal that even under the existed state systems like hv irradiation (LUMO system), no significant change happens in view of the type of interactions between the host and the drug. In addition, the GEDT indices for the sorbent in the adsorption process is about -0.180 which indicates that a small amount of electron charge transfer from the BUP drug to the MIP as sorbent.

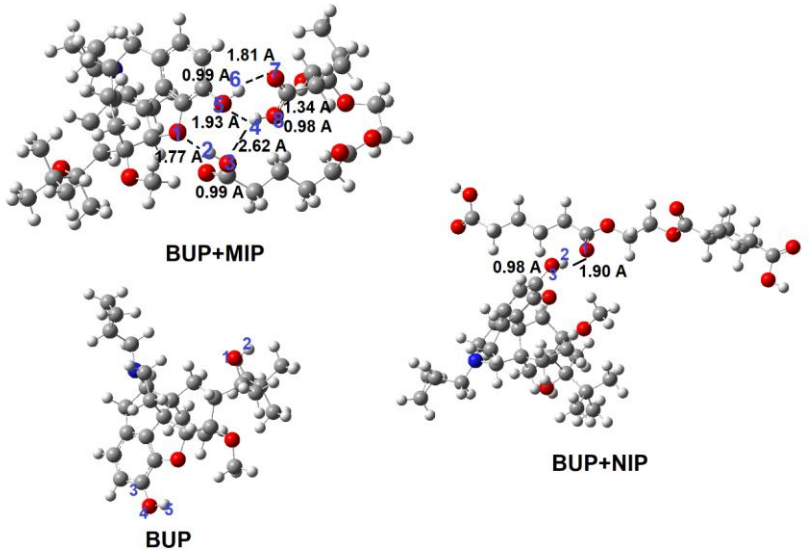

Figure 4. The geometrical structures for the isolated MIP, NIP, and BUP (drug), and the complex of sorbent-BUP systems optimized by quantum chemical calculations

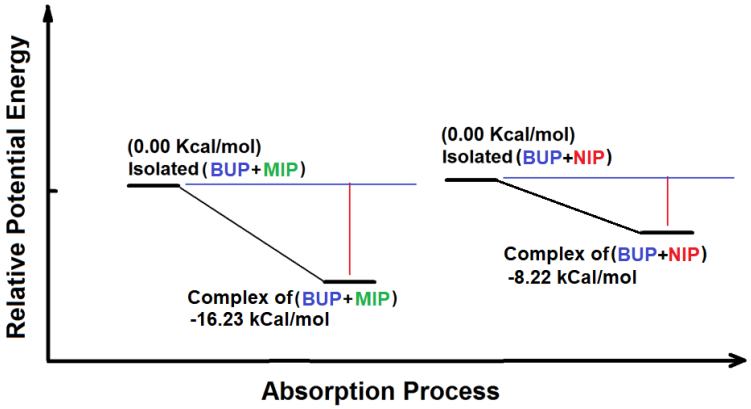

Figure 5. The potential energy surface (PES) of the absorption processes of BUP by the MIP as well as NIP calculated by the B3LYP quantum chemical method

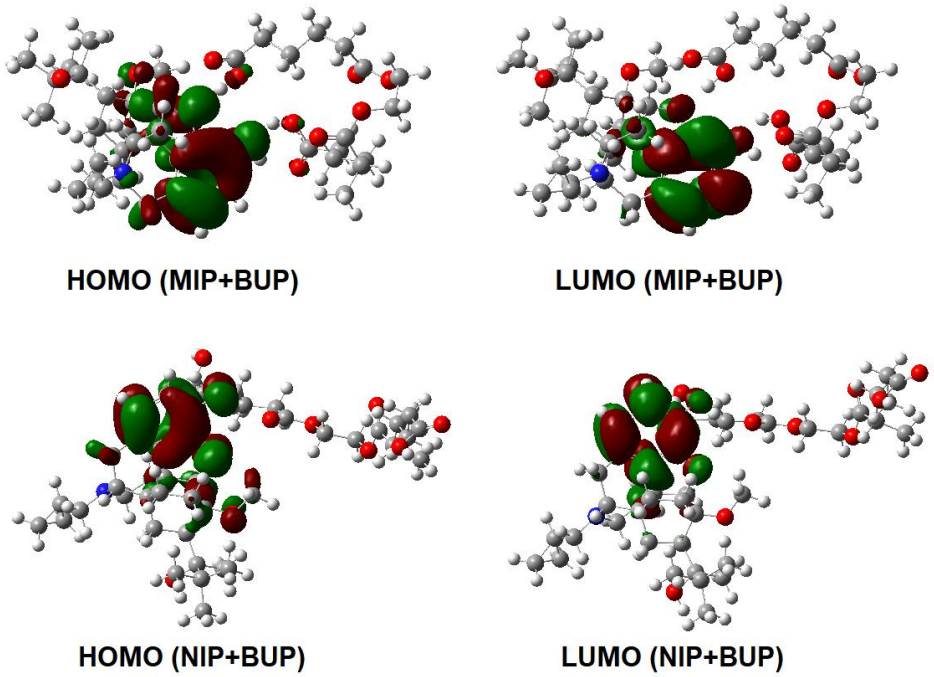

Figure 6. The Spatial distribution of FMOs of the complex of BUP with MIP, and with NIP

Conclusions

The results of this work showed that, a BUP templated MIP which could be obtained by precipitation/UV irradiation method, is able to adsorption this drug from the human blood plasma. Also, the results of the solid phase extraction which were monitored by HPLC-UV instrument revealed that the adsorption rate and value of BUP drug by MIP host are higher than that of NIP.

Finally, to study the adsorption behavior of BUP drug on the surface of the MIP, and NIP sorbents, we have applied the quantum chemical approaches. Thus, the sorbent-drug (as the guest-host) system was investigated by the DFT method. The results of the theoretical optimizations and the binding interactions indicated that there are several hydrogen bonds, as well as polar interactions between and the MIP-BUP system (which were considerably more than that of NIP-drug complex). Moreover, the PES data confirmed that the formation of MIP=BUP complex, releases a -16.32 kcal mol^{-1} of energy showing a spontaneous process in view of thermodynamics (which was more favorable than that of NIP-drug system with an energy release of -8.22 kcal mol^{-1}).

Experimental

Materials and reagents

All the chemicals and solvents were analytical grade. The ultra-pure water was prepared by a Milli-Q purification system (Millipore, Bedford, MA, USA). The compounds and reagents containing 2,2-azobisissobutyronitrile (AIBN), N-Methylmorpholine N-oxide (NMMO), N,N-dimethyl formamide (DMF), methacrylic acid (MAA)ethylene glycol dimethacrylate (EGDMA, 98% purity), and polycaprolactone-triol (PCL-T), were purchased from the Sigma-Aldrich company. Moreover, monobasic potassium phosphate (KH_2PO_4) methanol, and acetonitrile were prepared from the Merck Chemicals. In addition, the BUP active pharmaceutical ingredient (API) was bought from commercial sources, accordingly.

Instrumentation

The Shimadzu Prominence HPLC system (Shimadzu Corporation, Kyoto, Japan) equipped with a LC-20AD pump, a CTO-20A column oven, a DGU-20A degassing agent, and a SPD-20A UV-Vis detector, were used for the HPLC analyses. Moreover, the Lab-Solutions software version 5.51 was being employed for the data analysis and the other related processing. Also, an end-capped C18 ortho diesel silane (ODS), (250×4.6) mm, 5µm liquid chromatography column was applied for the assaying analysis of the concentration of BUP. Moreover, a CHZ-82 constant temperature water bath oscillator (Fuhua Instrument Co. Lid., China), a Spectrum 100 FT-IR spectrometer (PerkinElmer Co., Ltd., USA); a CR3i centrifuge (Thermo Fisher Scientific Inc., USA); a KQ2200B sonic device with frequency; a FEI Quanta 200 scanning electron microscope (Thermo Fisher Scientific, Netherland); and temperature controller (Kunshan Ultrosonic Instrument Co., Ltd., China) were applied for the related tasks. Finally, a ZRS-8G dissolution tester (Tianda Tianfa Technology Co., Ltd., China) was employed for the release examination.

Preparation of MIPs

Both of the prepared polymers containing the MIPs and NIPs (as the reference) were synthesized by the precipitation polymerization approach, and by using the UV photo polymerization, respectively. At the first step, 1mmol of BUP compound was dissolved in 75 ml of DMF as solvent. Then, 20 mmol of EGDMA, 4 mmol MAA, and 50 mmol of AIBN were respectively added to the mixture. Then, those were putted under the ultrasonic waves for about 10 min. Next, whole of the mixture was purged by nitrogen atmosphere for about 10 min [7-9]. After that, the reaction mixture was placed under UV irradiation at 366 nm for about 24 hours. Finally, the MIP, and NIP were being dried and grinned well for further use.

The obtained granules were powdered by grinding with a suitable mortar. Also, it should be mentioned that, the NIP was synthesized under the identical conditions without the existence of BUP as template. The schematic procedure for obtaining the MIP was presented in Figure **1**.

Characterization of the MIP composite

SEM analysis

The surface morphology of the composites was investigated by the SEM which its photographs were taken with a FEI ESEM QUANTA 200(USA). The cross-sections and surfaces of the MIPs and NIPs membranes were prepared by conductive deposition of the gold layer on the samples in a vacuum chamber. Figure 2 shows the SEM image of the membranes. In addition, the morphology of the samples was recorded under SEM scanning at the voltage of 25 kV, respectively.

FT-IR analysis

The FT-IR spectra of the MIP and the NIP were prepared by the FT-IR analyzer instrument. To do this, a certain portion (approximately about 5 mg) of the MIP and NIP granules along with a 100 mg powder of KBr were mixed well and then, were grind. Then, the mixture was pressed into a 1 mm pellets. The prepared samples were measured respectively on a Spectrum 100 FT-IR spectrometer. The FT-IR spectra of the MIP and the NIP were plotted by recording from 4000 to 400 cm^{-1} with a resolution of 2 cm^{-1} applying a pellet of KBr as the blank.

Friability of membranes

The physical strength of the composite was assessed by the Friability test. The NIPs and MIPs were rotated with friability device (Eraweka Abrasion Tester) with a speed of 25 rpm for 30 min. The friability of polymer was reached as the percentage of weight loss by following relation:

$$\text{friability } (as\ dryness) = \frac{(Wi - Wf)}{Wi} * 100 \quad (1)$$

According to the formula, W_i and W_f is the initial and the final weight of membranes.

Moisture Absorption

Before beginning the analysis, both of the MIP, and NIP were dried for about three days at room temperature. Then, in order to evaluate the swelling capacity of the composites, those were weighted and placed in a buffer at pH 7.4 for 6 hours at room temperature. Next, those were replaced and before weighting, the surface of composites was completely dried. The degree of swelling of the composites was reached, via relation 2:

$$\text{Moisture Absorption} = \left(\frac{(W2 - W1)}{W1}\right) * 100 \quad (2)$$

Where, W_1, W_2 are the MIP weights before, and after the swelling processes, respectively.

Data analysis

Adsorption experiments

In the case of the adsorption experiment, a 30.0 mg of the MIP or the NIP were suspended in 2 ml of

prepared plasma solution and a 10.0 mL of BUP solution (50 mg/L) between 2min – 240 min. Then, the sample solutions were filtered by a micro pored membrane, and the amount of the drug in filtrate was calculated by using the HPLC instrument according to the procedure describe in the HPLC section. The binding capacity of the MIP and the NIP and also the selectivity factor were obtained by Eq. (6) and Eq. (7), respectively.

$Qt = (C_0-C_t)V/m$ (6)

$\alpha = Q_{MIP}/Q_{NIP}$ (7)

where Q_t (μmol/g) is the adsorption capacity of the sorbent in different times, C_0 (mmol/L) is the initial concentration of BUP, Ct (mmol/L) is the concentration of BUP at time t, V (in Liter) is the volume of the initial BUP solution, and also, m is the mass of the NIP or the MIP (in g). Finally, α is the selectivity factor of the NIP to MIP, Q_{NIP} (μmol/g) is the adsorption capacity of NIP, and Q_{MIP} (μmol/g) is the adsorption capacity of the MIP.

HPLC method

The determination of the concentration and release the rate of BUP by using HPLC system was carried out by the Shimadzu HPLC system occupied with a UV/VIS detector set at 220 nm. The liquid chromatography (LC) separation was carried out by a C18 (4.6 mm, 250 mm, 5 μm) LC column. The injection volume was 20 μL, the flow rate was 1 ml/min and the temperature of the column camber was fixed at 25°C using the column oven. Also, an isocratic method was applied for the elusion and the mobile-phase was ACN/buffer solution with a 40/60, v/v percentage. Where, the buffer was prepared by dissolving the 10 mM of monobasic potassium phosphate in 1 liter of double distillated purified water set at pH of 2.5 by phosphoric acid [17-19].

Quantum chemical calculations

The isolated forms of BUP drug and the polymer of MAA- EGDMA were designed as input files and were then putted under optimization process to give the more stable energy minima. Next, the complexes of the sorbent in MIP, and NIP forms with the BUP drug were then designed and taken under theoretical calculations. The Gaussian 03 quantum chemical software was used to perform the required calculations [20]. Moreover, the key geometrical parameters were extracted accordingly. In addition, studies on all stationary points in addition to the other calculations were done by B3LYP/6-31g(d) level [21] which were confirmed to be trustable for such investigations [22]. The Global Electron Density Transfer (*GEDT*) were calculated using the following relation [23];

$GEDT=\Sigma q_A$ (7)

Where; q_A is the net Mulliken charge, as well as the sum of the all of the atoms of the gaseous species.

Moreover, the energy of adsorption E_{ad} was calculated by using the following relation [24-26]:

$E_{ad}=E_{sys}-(E_{Sorbent}+E_D)$ (8)

Where, E_{sys}, $E_{Sorbent}$, and E_D are the energy of the system, the energy of the isolated sorbent, and the energy of the drug, respectively.

Acknowledgment

The authors are grateful to Science and Research Branch of Islamic Azad University for all of their supports.

Declaration of Interests

The authors declare that there is not any conflict of interests.

References

[1] Guarnieri, M.; Kedda, J.; Tyler, B. *Cur. Med. Res. Opinion*, **2021**, *37*, 83.

[2] Ritvo, A. D.; Calcaterra, S. L; Ritvo, J. I. *J. Add. Med.*, **2021**, *15*, 252-4.

[3] Shah, K. H.; Makwana, R. P. *J. Drug Del. Therapeutic*s, **2021**, *11*, 201-204.

[4] Eriksson, A.; Jeppesen, S.; Krebs, L. *BMC Pregnancy Childbirth*, **2020**, *20*, 1.

[5] Behnia, N.; Azar, P. A.; Shekarchi, M.; Tehrani, M. S.; Adib, N. *Chem. Select*, **2022**, *7*, e202202553.

[6] Lee, H. Y.; Kim, H. E. Jeong, S. H. *Colloids Surf. B Biointerfaces*, **2019**, *174*, 308.

[7] Yahyapour, M.; Ranjbar, M.; Mohadesi, A.; Rejaeinegad, M. *Electroanalysis*, **2022**, *34*, 1012-1020.

[8] a) Ganjavi, F.; Ansari, M.; Kazemipour, M.; Zeidabadinejad, L. *J. Sep. Sci.*, **2017**, *40*, 3175; b) Habibi, B.; Rostamkhani, S.; Hamidi, M. *J. Iran. Chem. Soc.*, **2018**, *15*, 1569.

[9] Gokulakrishnan, K.; Prakasam, T. *Arab. J. Chem.* **2016**, *9*, S528.

[10] Panahi, Y.; Motaharian, A.; Hosseini, M. R. M.; Mehrpour, O. *Sensors Actuators B: Chem.* **2018**, *273*, 1579-1586.

[11] Rezaei, M.; Rajabi, H. R.; Rafiee, Z. *Colloids and Surfaces A: Physicochemical and Engineering Aspects*, **2020**, *586*, 124253.

[12] Cieplak, M.; Kutner, W. *Trends Biotech.* **2016**, *34*, 922.

[13] Wang, Z.; Duan, Y.; Duan, Y. *J. Cont. Release*, **2018**, *290*, 56.

[14] Tryfonidou, M. A.; de Vries, G.; Hennink, W. E.; Creemers, L. B. *Adv. Drug Del. Rev.*, **2020**, *160*, 170.
[15] Jun, X. U.; Wang, X. Y.; Guo, W. Z. *J. Integrative Agricul.*, **2015**, *14*, 1673.
[16] Karameta, E.; Gourgouliani, N.; Kouvari-Gaglia, D.; Litsi-Mizan, V.; Halle, S.; Meiri, S.; Sfenthourakis, S.; Pafilis, P. *J. Linnean Soc.*, **2017**, *121*, 883-893.
[17] a) Siadati, S. A.; Rezvanfar, M. A.; Payab, M.; Beheshti, A. *Curr. Chem. Lett.*, **2021**, *10*, 151; b) Beheshti, A.; Kamalzadeh, Z.; Haj-Malek, M.; Payab, M.; Rezvanfar, M.; Siadati, S. A. *Curr. Chem. Lett.*, **2021**, *10*, 281.
[18] Alves, A. C.; Ramos, I. I.; Nunes, C.; Magalhães, L. M.; Sklenářová, H.; Segundo, M. A.; Reis, S. *Talanta*, **2016**, *146*, 369-374.
[19] a) Seo, J. E.; Kim, S.; Kim, B. H. *J. Exposure Sci. Environ. Epidem.* **2017**, *27*, 320-325.; b) Dadras, A.; Rezvanfar, M. A.; Beheshti, A.; Naeimi, S. S.; Siadati, S. A. *Comb. Chem…& High Throughput Scr.* **2022**, *25*, 838-846.
[20] Frisch, et al., M. J. Gaussian 03. Revision A, **2003**.
[21] Zeroual, A.; Benharref, A.; El Hajbi, A. *J. Mol. Mod.*, **2015**, *21*, 1.
[22] Siadati, S. A.; Amini-Fazl, M. S.; Babanezhad, E. *Sens. Actuators B: Chem.* **2016**, *237*, 591-596.
[23] Mohtat, B.; Siadati, S. A.; Khalilzadeh, M. A.; Zareyee, D. *J. Mol. Struc.* **2018**, *1155*, 58-64.
[24] a) Nasiri, A.; Khalilzadeh, M. A.; Zareyee, D. *J. Coord. Chem.* **2022**, *75*, 256; b) Pakravan, P.; Siadati, S. A. *J. Mol. Graph. Mod.* **2017**, *75*, 80.
[25] a) Siadati, S. A.; Mirabi, A. *Prog. Reac. Kinet. Mech.* **2015**, *40*, 383; b) Siadati, A. *Lett. Org. Chem.* **2016**, *13*, 2.
[26] a) Mohtat, B.; Siadati, S. A.; Khalilzadeh, M. A. *Prog. Reac. Kinet. Mech.* **2019**, *44*, 213; b) Rostamian, R.; Khalilzadeh, M. A.; Zareyee, D. *Sci. Rep.* **2022**, *12*, 1.